Effects of seasonal variation of photosynthetic capacity on the carbon fluxes of a temperate deciduous forest

David Medvigy,[1] Su-Jong Jeong,[1] Kenneth L. Clark,[2] Nicholas S. Skowronski,[3] and Karina V. R. Schäfer[4]

Received 17 June 2013; revised 14 November 2013; accepted 16 November 2013.

[1] Seasonal variation in photosynthetic capacity is an important part of the overall seasonal variability of temperate deciduous forests. However, it has only recently been introduced in a few terrestrial biosphere models, and many models still do not include it. The biases that result from this omission are not well understood. In this study, we use the Ecosystem Demography 2 model to simulate an oak-dominated stand in the New Jersey Pine Barrens. Two alternative model configurations are presented, one with seasonal variation of photosynthetic capacity (SPC-ON) and one without seasonal variation of photosynthetic capacity (SPC-OFF). Under typical climate conditions, the two configurations simulate values of monthly gross primary productivity (GPP) as different as 0.05 kg C m^{-2} $month^{-1}$ in the early summer and 0.04 kg C m^{-2} $month^{-1}$ in the fall. The differences between SPC-ON and SPC-OFF are amplified when there is temporal correlation between photosynthetic capacity and climate anomalies or disturbances. Warmer spring temperatures enhance GPP in SPC-ON more than in SPC-OFF, but warmer fall temperatures enhance GPP in SPC-OFF more than in SPC-ON. Defoliation by gypsy moth, a class of disturbance that typically happens in late spring in the New Jersey Pine Barrens, has a disproportionately negative impact on GPP in SPC-ON. It is concluded that including seasonal variation of photosynthetic capacity in models will improve simulations of monthly scale ecosystem functioning as well as of longer-term responses to climate change and disturbances.

Citation: Medvigy, D., S.-J. Jeong, K. L. Clark, N. S. Skowronski, and K. V. R. Schäfer (2013), Effects of seasonal variation of photosynthetic capacity on the carbon fluxes of a temperate deciduous forest, *J. Geophys. Res. Biogeosci.*, *118*, doi:10.1002/2013JG002421.

1. Introduction

[2] Phenology refers to the study of the timing of seasonally recurring biological events. In temperate forests, seasonal variation of leaf area is one obvious and important aspect of phenology [*Richardson et al*., 2013]. However, there are other aspects of phenology that warrant attention. In particular, seasonal variation of leaf photosynthetic capacity has been shown to affect the functioning of temperate deciduous forests [*Wilson et al*., 2001; *Xu and Baldocchi*, 2003; *Grassi et al*., 2005; *Wang et al*., 2008; *Ow et al*., 2010] and temperate grasslands [*Wolf et al*., 2006]. In a synthesis of observations, *Bauerle et al*. [2012] argued that seasonal variation of photosynthetic capacity for broadleaf deciduous trees was related to photoperiod, with photosynthetic capacity attaining a maximum around the summer solstice and then declining in concert with photoperiod. Although seasonal variation in photosynthetic capacity has been incorporated into a few terrestrial biosphere models [*Krinner et al*., 2005; *Medvigy et al*., 2009; *Oleson et al*., 2010], the specifics of the implementations have varied, and many models have not included it at all. Consequently, the broad implications of the seasonal variation of photosynthetic capacity are not well understood.

[3] The impacts of seasonal variation in photosynthetic capacity are likely to be sensitive to particular time scales. Consider a pair of forest stands, one of which has a seasonal variation of photosynthetic capacity that tracks photoperiod, and the other without seasonal variation of photosynthetic capacity (Figure 1). We propose here that it is possible for these two types of stands to yield, on average, similar annual gross primary productivity (GPP) but different monthly GPP. The essential prerequisite for this is that the stand with seasonal variation of photosynthetic capacity must have a larger maximum photosynthetic capacity than the stand without seasonal variation in photosynthetic capacity. Then, the stand that experiences seasonal variation in photosynthetic capacity would have less GPP during the spring and fall than a

[1]Department of Geosciences, Princeton University, Princeton, New Jersey, USA.
[2]Silas Little Experimental Forest, USDA Forest Service, New Lisbon, New Jersey, USA.
[3]USDA Forest Service, Northern Research Station, Morgantown, West Virginia, USA.
[4]Department of Biological Sciences, Rutgers University, Newark, New Jersey, USA.

Corresponding author: D. Medvigy, Department of Geosciences, Guyot Hall, Princeton University, Princeton, NJ 08544, USA. (dmedvigy@princeton.edu)

2169-8953/13/10.1002/2013JG002421

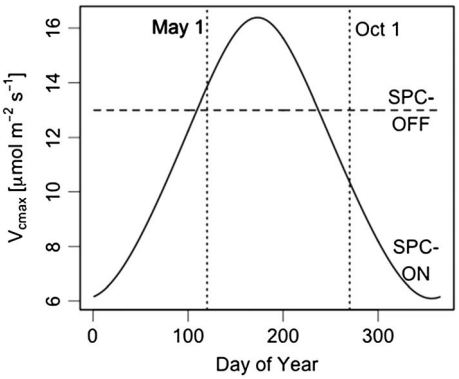

Figure 1. Seasonal changes in V_{cmax} at 25°C using our best estimates for model parameters (Table 3). The V_{cmax} in SPC-ON (solid line) depends on photoperiod while the V_{cmax} from SPC-OFF (horizontal dashed line) does not. The vertical dotted lines, placed at 1 May and 1 October, approximate the start and end of the growing season.

stand with constant photosynthetic capacity, more GPP in early summer, and similar annual average GPP.

[4] Here, we present three hypotheses based on these ideas. (1) If unfavorable climate anomalies were more likely to occur during times of long photoperiod, the GPP of seasonal photosynthetic capacity trees will be affected more strongly than that of constant photosynthetic capacity trees. Conversely, unfavorable climate anomalies occurring during times of short photoperiod will have less of an effect on the GPP of seasonal photosynthetic capacity trees than that of constant photosynthetic capacity trees. (2) Certain disturbances, such as defoliation by insects, tend to occur at particular times of the year. In the forests of the eastern US Atlantic coastal plain, defoliation by gypsy moth (*Lymantria dispar* L.) larvae tends to occur during times of relatively long photoperiod [*Liebhold et al*., 1992; *Johnson et al*., 2005, 2006]. Consequently, seasonal photosynthetic capacity trees will be more strongly affected by defoliation than constant photosynthetic capacity trees. (3) There will be interactions between seasonal variations of leaf area and seasonal variations of photosynthetic capacity. If global warming causes earlier budburst or delayed senescence [*Menzel et al*., 2008; *Lebourgeois et al*., 2010; *Vitasse et al*., 2011; *Migliavacca et al*., 2012; *Jeong et al*., 2013], the ability of vegetation to capitalize on the prolonged growing season and increase carbon uptake will hinge on photosynthetic capacity being sufficiently high at the start and end of the growing season. Thus, the carbon gains achieved by trees with seasonal variations of photosynthetic capacity will be less than the gains achieved by trees with constant photosynthetic capacity if increasing temperatures cause growing seasons to be lengthened.

[5] In this paper, we test these ideas using model simulations of a highly instrumented forested stand in the New Jersey Pinelands. In section 2, we describe the model, the forest stand, and the simulation design. In section 3, we evaluate model performance and assess how seasonal variations in photosynthetic capacity modulate the impacts of transient climate anomalies, defoliation, and increased temperatures. Section 4 contains a discussion of our results, and our conclusions are presented in section 5.

2. Methods

2.1. Model Description

[6] Our model simulations were carried out with the Ecosystem Demography 2 model (ED2). Although ED2 is a regional model, it is used here in single-grid cell mode because we are interested in understanding processes rather than regional variations. The grid cell is intended to represent the approximate footprint of an eddy flux tower (1 km^2). Detailed descriptions of ED2 already exist in the literature [*Medvigy et al*., 2009; *Medvigy and Moorcroft*, 2012]. Here we give a brief overview of the most relevant aspects of the model, including those related to photosynthetic capacity. For further details, see *Medvigy et al*. [2009].

[7] ED2 distinguishes different resource environments, and, in each resource environment, tracks the number density of trees of different sizes and plant functional types [Medvigy et al., 2009; *Medvigy and Moorcroft*, 2012]. Forest structure and composition can be initialized directly from forest census information. Each tree observed in an actual measurement plot has a direct representation in ED2. On subdaily time scales, tree-level GPP and net primary production (NPP) are calculated using parameterizations for radiative transfer, leaf biophysics, photosynthesis, and respiration [*Medvigy et al*., 2009]. When integrated over time, tree-level GPP and NPP determine tree growth, mortality, and reproduction. Tree diameter is a prognostic variable in the model and it is connected to maximum tree leaf area index (LAI) through allometric relationships (Appendix A). Site-level LAI evolves in time as trees grow, die, and reproduce.

[8] Two options for photosynthetic capacity were implemented. The first option is the conventional one, in which the maximum rate of carboxylation (V_{cmax}) depends on temperature, but does not otherwise have any seasonal dependence:

$$V_{cmax} = V_{cmax,s} \frac{e^{3000(1/288.15-1/T)}}{(1+e^{0.4(277.85-T)})(1+e^{0.4(T-318.15)})}. \quad (1)$$

[9] In equation (1), $V_{cmax,s}$ is a constant and T is the leaf temperature in K. The factors in the denominator ensure that V_{cmax} approaches 0 as temperatures get very low or very high. The second option includes seasonal variation of photosynthetic capacity according to the formulation of *Oleson et al*. [2010], who introduced a quadratic dependence of V_{cmax} on photoperiod (P):

$$V_{cmax} = V_{cmax,s} \left(\frac{P}{P_s}\right)^2 \frac{e^{3000(1/288.15-1/T)}}{(1+e^{0.4(277.85-T)})(1+e^{0.4(T-318.15)})}. \quad (2)$$

[10] P itself depends on day-of-year and latitude [*Bonan*, 2008]. The photoperiod at the summer solstice is denoted P_s. At a given temperature, equation (2) states that V_{cmax} takes on its largest value at the summer solstice, declines between the summer solstice and the winter solstice, and then increases from the winter solstice to the summer solstice (Figure 1).

2.2. Model Initialization and Forcing

[11] We used an intermediate-aged upland forest stand in the New Jersey Pinelands as a test bed for our analysis. This stand is located in the Silas Little Experimental Forest (SLEF) and is oak dominated with a small amount of pine.

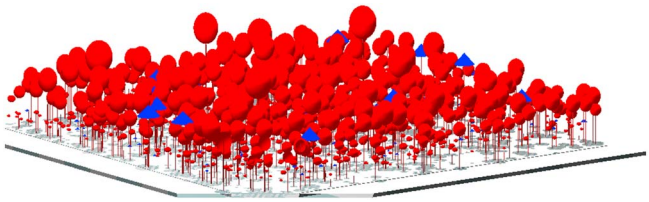

Figure 2. Representation of forest structure and composition in the ED2 model derived from inventory measurements at the Silas Little Experimental Forest. Red colors represent oaks and blue colors represent pines.

An earlier version of ED2 has already been evaluated for this stand [*Medvigy et al*., 2012]. Detailed descriptions of the stand can be found in *Clark et al*. [2010, 2012]; here we review only the data sets that are most relevant to the present study.

[12] Measurements of stand structure and composition, soil carbon, litter, and woody debris [*Skowronski et al*., 2007; *Clark et al*., 2010; *Schäfer*, 2011] were used to initialize the model. All oaks were mapped into a single oak plant functional type (PFT) and all pines were mapped into a single pine PFT. The resulting forest structure and composition are shown in Figure 2. Except as specified in Appendix A, the oak PFT was the same as the ED2 mid-successional hardwood, and the pine PFT was the same as the ED2 northern pine [*Medvigy et al*., 2009]. Meteorological measurements have been made from an overstory (19 m) tower at SLEF since 2005 [*Clark et al*., 2010, 2012] and were used to force the model. The required measurements included incoming photosynthetically active radiation (PAR), incoming longwave radiation, air temperature, relative humidity, wind speed, pressure, and precipitation. An eddy covariance system is also located on the tower and has been providing measurements of net ecosystem exchange (NEE; net flux of CO_2 between the land and the atmosphere) since 2005 [*Clark et al*., 2010, 2012].

[13] Herbivory by gypsy moth was observed to reduce the total leaf area index (LAI) to less than 0.5 $m^2\ m^{-2}$ during the early summer of 2007 [*Clark et al*., 2010, 2012; *Schäfer et al*., 2010]. Following the peak of herbivory in mid-June, a second, partial leaf-out occurred and resulted in a total LAI of about 50% of the maximum LAI occurring in 2005 and 2006. In 2008, partial defoliation reduced canopy LAI again, although a second leaf-out did not occur. The timing of defoliation has been reconstructed using sap flux, litter, and frass measurements [*Schäfer et al*., 2010], and has previously been implemented into ED2 as a prescribed disturbance [*Medvigy et al*., 2012].

2.3. Model Experiments

[14] We developed two model configurations that made different assumptions about the seasonality of photosynthetic capacity. In our "SPC-OFF" configuration, we used the conventional approach in which V_{cmax} depended on temperature but did not depend on photoperiod (equation (1)). In our "SPC-ON" configuration, V_{cmax} had the same temperature dependence as in SPC-OFF, but also had a quadratic dependence on photoperiod (equation (2)).

2.3.1. Model Optimization and Evaluation

[15] We used Markov chain Monte Carlo to estimate several model parameters in both the SPC-OFF and SPC-ON configurations. Markov chain Monte Carlo has previously been used to constrain terrestrial biosphere models [*Knorr and Kattge*, 2005; *Richardson and Hollinger*, 2005; *Richardson et al*., 2010; *Trudinger et al*., 2007; *Fox et al*., 2009; *Jeong et al*., 2012]. The joint probability distribution of four parameters was estimated for the SPC-OFF and SPC-ON configurations. Details on our Markov chain Monte Carlo implementation can be found in Appendix A.

[16] We used our Markov chain Monte Carlo results to create an ensemble of possible parameter sets for the SPC-OFF and SPC-ON configurations. In both cases, we first identified the parameter set that maximized the posterior probability density function. We then randomly sampled the posterior probability density function nine times. This led to a total of 10 parameter sets for both the SPC-OFF and the SPC-ON configurations.

[17] The full period for which data are currently available (2005–2011) was simulated using these parameter sets. We denote these ensembles "SPC-OFF-EVAL" and "SPC-ON-EVAL" for the SPC-OFF and SPC-ON configurations, respectively (Table 1). For each ensemble, we computed the ensemble mean of each predicted quantity. We characterized the spread in model predictions by computing the standard deviation of the predictions of all ensemble members. This approach allowed us to assess the impacts of parameter uncertainty. The ability of each ensemble to simulate the observed eddy fluxes and tree growth and mortality was then evaluated.

2.3.2. Impacts of Seasonal Variation of Photosynthetic Capacity

[18] We carried out longer-term simulations using the same parameter sets to further highlight the differences between the SPC-OFF and SPC-ON configurations (Table 1). These simulations ran for 42 years. The meteorological forcings for the 42 years were created by repeatedly cycling over the 7 years of

Table 1. Ensembles Carried Out as Part of this Study

Name	Seasonal variation of Photosynthetic Capacity	Years Simulated	Meteorological Forcing	Defoliation
SPC-OFF-EVAL	No	2005–2011	2005–2011	2007 only
SPC-OFF-LONG	No	42 years	2005–2011	None
SPC-OFF-DEF	No	42 years	2005–2011	Year 3 only
SPC-OFF-WARM	No	42 years	(2005–2011) + 4°C	None
SPC-ON-EVAL	Yes	2005–2011	2005–2011	2007 only
SPC-ON-LONG	Yes	42 years	2005–011	None
SPC-ON-DEF	Yes	42 years	2005–2011	Year 3 only
SPC-ON-WARM	Yes	42 years	(2005–2011) + 4°C	None

Table 2. Weighted Log Likelihoods (w_i LL_i) for Different Model Formulations

Data Set	SPC-OFF	SPC-ON
Half-hourly gapped NEE	−1.4	−0.8
Monthly gapped NEE	−288.2	−205.0
Monthly nighttime gapped NEE	−105.7	−100.3
Yearly gapped NEE	−5.6	−2.8
Yearly nighttime gapped NEE	−11.7	−7.1
Basal area growth, oaks	−1.9	−3.1
Basal area growth, pines	−0.1	−0.1
Basal area mortality, oaks	−1.5	−1.6
Basal area mortality, pines	−15.8	−17.7
Total	−431.9	−338.5

meteorological observations (2005–2011). This simulation length allowed an adequate amount of time for the model to equilibrate after disturbances such as gypsy moth attack and warming perturbations (see below). All simulations were initialized with the 2005 forest composition (Figure 2). For simplicity, we focused our analysis on model predictions of GPP because of the close association between GPP and photosynthetic capacity. All simulations were forced with the same solar radiation, and so solar radiation is controlled for in comparisons between SPC-OFF and SPC-ON.

2.3.2.1. Direct Effects of Seasonal Variation of Photosynthetic Capacity

[19] The objectives of these simulations were to determine the long-term differences in GPP between the SPC-OFF and SPC-ON configurations, determine the differences in the average seasonal cycle, and to identify any differential impacts of climate anomalies. Ten simulations were carried out for each configuration, corresponding to the parameter sets used in SPC-OFF-EVAL and SPC-ON-EVAL. The SPC-OFF simulations were denoted "SPC-OFF-LONG" and the SPC-ON simulations were denoted "SPC-ON-LONG" (Table 1). No defoliation was implemented in these simulations.

[20] For any quantity, we calculated the pure effect of seasonal variation of photosynthetic capacity by taking the difference between SPC-ON-LONG and SPC-OFF-LONG. We expected that the effect on GPP would be correlated with climate, but assessing the statistical significance of the correlation was not straightforward because the periodic meteorological forcing led to strong autocorrelation in our simulation results, reducing the effective degrees of freedom. To account for this, we averaged overall simulation results conditional on the meteorological forcing before computing the correlations. This generated a time series of 7 years duration, matching the length of the observational record. Correlations between the pure effects of seasonal variation of photosynthetic capacity and monthly solar radiation, temperature, and soil water were then assessed using Spearman's ρ, a nonparametric measure of correlation.

2.3.2.2. Effects of Defoliation

[21] We created "SPC-ON-DEF" and "SPC-OFF-DEF" ensembles that were identical to SPC-ON-LONG and SPC-OFF-LONG, respectively, in every way except for the disturbance forcing. In the third year of SPC-ON-DEF and SPC-OFF-DEF, we prescribed a defoliation event according to the observed 2007 defoliation [*Medvigy et al*., 2012]. No other defoliation was prescribed in the remainder of the simulations (Table 1). The pure effects of seasonal variation of photosynthetic capacity, the pure effects of defoliation, and the nonlinear interaction term were distinguished according to:

$$\text{Pure Photosynthetic Capacity} = \text{SPC-ON-LONG minus SPC-OFF-LONG;} \quad (3a)$$

$$\text{Pure Defoliation} = \text{SPC-OFF-DEF minus SPC-OFF-LONG;} \quad (3b)$$

$$\text{Interaction} = (\text{SPC-ON-DEF minus SPC-ON-LONG}) \text{ minus } (\text{SPC-OFF-DEF minus SPC-OFF-LONG}). \quad (3c)$$

2.3.2.3. Effects of Increased Temperature

[22] We investigated the effects of increased temperature by carrying out two additional ensembles, "SPC-ON-WARM" and "SPC-OFF-WARM," that were identical to SPC-ON-LONG and SPC-OFF-LONG, respectively, in every way except for the meteorological forcing (Table 1). Warming was implemented by increasing all temperatures by 4°C. This increase is at the upper end of climate model projections for 2100 [*Meehl et al*., 2007]. All other meteorological driver variables (PAR, longwave radiation, relative humidity, precipitation, pressure, wind speed) were kept the same. Although future climate change may also lead to changes in these other variables [*Seager et al*., 2013], climate models disagree on how they will change. We therefore decided to focus on the case of a simple temperature increase. The pure effects and interaction term were calculated using a procedure analogous to equation (3).

3. Results

3.1. Model Optimization and Evaluation

[23] The SPC-ON configuration achieved a better overall fit to the NEE measurements and tree biometry measurements than the SPC-OFF configuration (Table 2). The differences occurred mainly in the simulations of monthly gapped NEE. The gapped NEE includes only the NEE values that were actually observed and passed quality-control (see Appendix A). Predictions of yearly gapped NEE were only slightly better in SPC-ON than in SPC-OFF, indicating that the errors accrued by SPC-OFF in the monthly gapped NEE largely canceled out when summed over all months. The two model configurations also gave similar results for annual growth

Table 3. Parameter Values Corresponding to the Maximum of the Posterior Probability Density Function[a]

Parameter	Symbol	Units	SPC-OFF	SPC-ON
Maximum rate of carboxylation at summer solstice at 15°C	$V_{cmax,s}$	$\mu mol\ m^{-2}\ s^{-1}$	13.0 (0.3)	16.4 (0.3)
Fine root turnover rate	T_{root}	a^{-1}	2.0 (0.1)	1.9 (0.2)
Slope of stomatal conductance-photosynthesis relationship	M	-	42 (1)	35 (3)
Baseline heterotrophic respiration rate	$\alpha_{sx}/\alpha_{sx,orig}$	-	1.06 (0.09)	1.20 (0.05)

[a]Standard errors are shown in parentheses.

Table 4. Evaluation of ED2 at the Silas Little Experiment Forest

Data Set	Units	Observations	Bias: SPC-OFF	RMS Error: SPC-OFF	Bias: SPC-ON	RMS Error: SPC-ON
Annual gapped NEE[a]	tC ha^{-1} y^{-1}	−2.35	−0.22	0.95	0.03	0.81
Monthly gapped NEE[a]	tC ha^{-1} $month^{-1}$	−0.196	−0.018	0.24	0.002	0.22
Oak basal area growth[b]	cm^2 m^{-2}	1.1	−0.2	n.a.	0.1	n.a.
Pine basal area growth[b]	cm^2 m^{-2}	0.1	−0.1	n.a.	−0.1	n.a.
Oak basal area mortality[b]	cm^2 m^{-2}	5.6	−0.2	n.a.	0.4	n.a.
Pine basal area mortality[b]	cm^2 m^{-2}	0.0	0.9	n.a.	0.5	n.a.

[a]Includes years 2005–2011.
[b]Difference between autumn 2009 and autumn 2005.

and mortality, although SPC-OFF was slightly better than SPC-ON for these quantities.

[24] The parameter sets that maximized the posterior probability density functions for SPC-OFF and SPC-ON are given in Table 3 (see Appendix A for parameter definitions). Because the $V_{cmax,s}$ from SPC-ON was larger than the $V_{cmax,s}$ from SPC-OFF, the SPC-ON simulations have larger values of $V_{cmax,s}$ than SPC-OFF around the times of the longest photoperiod (June–July), and smaller values during the fall (September–October). The resulting seasonal cycles of V_{cmax} are shown in Figure 1. The difference in V_{cmax} seasonality between SPC-ON and SPC-OFF leads to differences in the seasonality of gapped NEE, and also explains how relatively low mid-summer values of V_{cmax} in SPC-OFF can be compensated for by high values in the fall, thus leading to an annual average carbon uptake that is similar to that of SPC-ON. The percent difference for $V_{cmax,s}$ (26%) between the SPC-ON and SPC-OFF values was larger than the percent difference for any of the other estimated parameters.

[25] SPC-ON-EVAL was a closer match to almost all target data sets than SPC-OFF-EVAL during the 2005–2011 evaluation period (Table 4). In particular, for the gapped yearly and monthly NEE, the biases associated with SPC-ON-EVAL were almost an order of magnitude smaller than those of SPC-OFF-EVAL. Model performance in each month is shown in Figure 3a, which compares the gapped monthly NEE for the observations, SPC-OFF-EVAL, and SPC-ON-EVAL. In almost all years, SPC-ON-EVAL is better than SPC-OFF-EVAL in simulating the maximum summer drawdown. The main exception to this is 2007, the year of the gypsy moth outbreak. Overall monthly biases and RMSEs over 2005–2011 are shown in Figures 3b and 3c, respectively. Both SPC-ON-EVAL and SPC-OFF-EVAL exhibit similar positive biases in May (Figure 3b), suggesting that budburst may be occurring too late in all simulations. SPC-OFF-EVAL also has large negative biases in September–October, while the biases from SPC-ON-EVAL are near zero in these months (Figure 3b). RMSEs are smaller in SPC-ON-EVAL

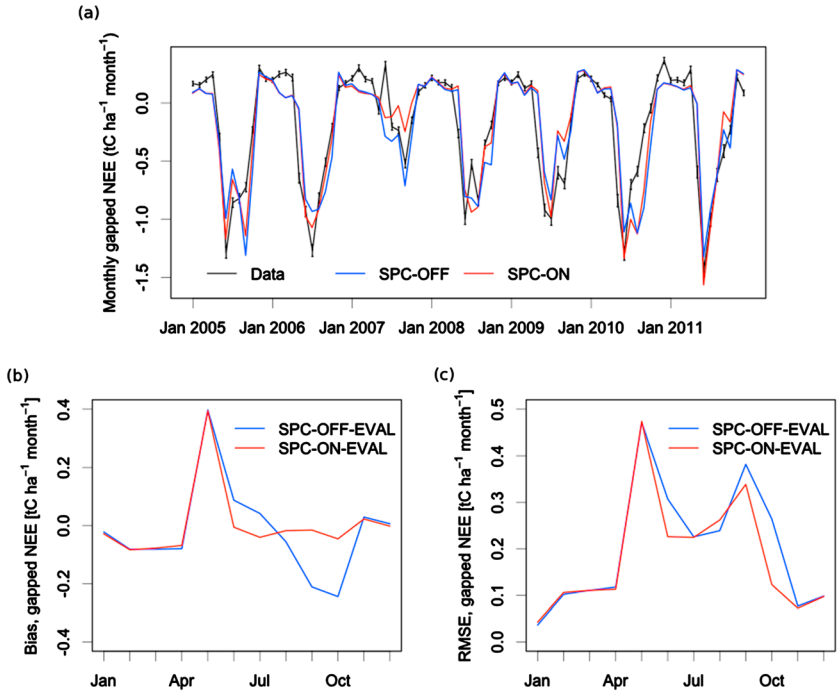

Figure 3. Evaluation of model performance over 2005–2011 at SLEF. Panel (a): Time series of gapped monthly NEE from the observations and the ensemble means from SPC-OFF-EVAL and SPC-ON-EVAL. Error bars denote the 95% confidence interval for the observations. Panel (b): Ensemble-mean model bias, conditional on month. Panel (c): Ensemble-mean model RMSE, conditional on month.

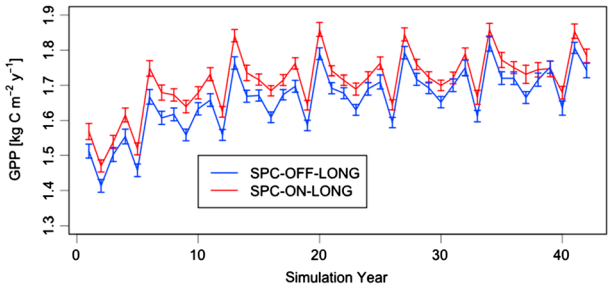

Figure 4. Annual mean gross primary productivity (GPP) from our simulations with seasonal variation of photosynthetic capacity (SPC-ON-LONG) and without seasonal variation of photosynthetic capacity (SPC-OFF-LONG). The solid lines show the ensemble means and the errors bars show plus and minus 1 ensemble standard deviation.

than in SPC-OFF-EVAL in June, September, and October, but are slightly larger in August (Figure 3c). Tree basal area growth and mortality for 2005–2009 were simulated comparably well by both model configurations, including the large amount of mortality in the years following defoliation (Table 4).

3.2. Direct Effects of Seasonal Variation of Photosynthetic Capacity

[26] Annual GPP is shown in Figure 4 for SPC-ON-LONG and SPC-OFF-LONG. In both ensembles, annual GPP steadily increased over the first 10–15 years and then stabilized at values that were about 10% greater than those at the beginning of the simulation. There was a 7 year periodicity in annual GPP associated with the periodicity of the meteorological forcing. In each year, the ensemble mean GPP from SPC-ON-LONG exceeded that of SPC-OFF-LONG. The percent differences were initially about 4% and were generally separated by more than 1 ensemble standard deviation. By the end of the simulation, the difference between the ensemble means was reduced to about 2% and there were more and more years in which the ensemble standard deviations overlapped.

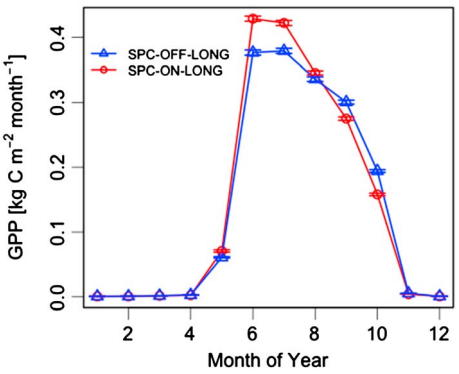

Figure 5. Average annual cycle of gross primary productivity (GPP) from our simulations with seasonal variation of photosynthetic capacity (SPC-ON-LONG) and without seasonal variation of photosynthetic capacity (SPC-OFF-LONG). The solid lines show the ensemble means and the errors bars show plus and minus 1 ensemble standard deviation.

[27] We computed the average annual cycle to determine the months when SPC-ON-LONG had greater GPP than SPC-OFF-LONG (Figure 5). The largest differences were in early summer and in fall. In June and July, SPC-ON-LONG had about 12% greater GPP than SPC-OFF-LONG. These are months with long photoperiod, and photosynthetic capacities in SPC-ON-LONG are larger than those in SPC-OFF-LONG (Figure 1). Conversely, in September and October, photoperiods are relatively short, and SPC-OFF-LONG has a larger photosynthetic capacity and 15% greater GPP than SPC-ON-LONG. In May and August, photosynthetic capacities in the two model configurations are nearly equal, and GPP differences are small. GPP differences are also small from November through April, when deciduous trees do not have leaves.

[28] In June, there was a statistically significant positive correlation between solar radiation and the "SPC-ON-LONG minus SPC-OFF-LONG" GPP difference (Table 5). In September, there was a statistically significant negative correlation between these variables (Table 5). These results are consistent with our expectation that positive radiation anomalies would have a stronger impact when there are larger photosynthetic capacities. Positive temperature anomalies also favored SPC-ON-LONG over SPC-OFF-LONG in May and June (Table 5). V_{cmax} is an increasing function of temperature for typical May–June temperatures at SLEF (equation (1)), and so photosynthesis should be positively correlated with temperature during these months. Because V_{cmax} is larger in SPC-ON-LONG than in SPC-OFF-LONG during these months (Figure 1), SPC-ON-LONG showed a greater increase in GPP during positive temperature anomalies.

[29] In December–January–February, positive temperature anomalies favored the GPP in SPC-OFF-LONG over SPC-ON-LONG (Table 5). This GPP difference was due to the small amount of pines present in both simulations. Averaged over the simulations, pine leaf area index (LAI) was 14% larger in SPC-OFF-LONG than in SPC-ON-LONG. Because of this difference in pine LAI, SPC-OFF-LONG was able to have a larger response to winter temperature anomalies than SPC-ON-LONG. However, absolute values of GPP were very small in both simulations during these months (Figure 5). We did not find a statistically significant correlation between GPP difference and soil water in any month.

3.3. Interaction With Defoliation

[30] The simulated impact of a single complete defoliation event on annual GPP is shown in Figure 6a. In the year of defoliation itself, annual GPP in SPC-OFF-DEF was only about 50% that of SPC-OFF-LONG. Annual GPP in SPC-

Table 5. Statistically Significant ($p < 0.05$) Correlations Between Monthly "SPC-ON-LONG Minus SPC-OFF-LONG" GPP Difference and Monthly Climate Drivers

Climate Driver	Month	Spearman's ρ	p-Value
Solar radiation	June	0.96	0.003
Solar radiation	September	−0.96	0.003
Temperature	January	−0.96	0.003
Temperature	February	−0.93	0.007
Temperature	May	0.86	0.02
Temperature	June	0.89	0.01
Temperature	December	−0.96	0.003

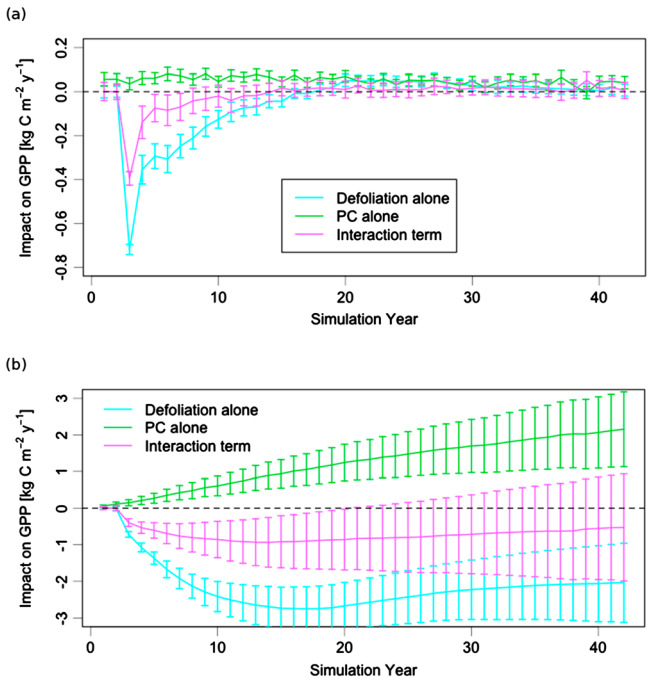

Figure 6. Impacts of insect defoliation and seasonal variation of photosynthetic capacity. Panel a: Impacts on annual gross primary productivity (GPP). Panel b: Cumulative impacts on GPP. In both panels, the solid lines show the ensemble means and the errors bars show plus and minus 1 ensemble standard deviation.

OFF-DEF recovered over the next 15 years and eventually reached levels similar to SPC-OFF-LONG. There were also years in which the interaction term (equation (3c)) was important. In the year of defoliation (simulation year 3), its magnitude was about half that of the pure effect of defoliation. This was consistent with our expectation that disturbances taking place in early summer would impact the SPC-ON configuration more strongly than the SPC-OFF configuration. However, this effect was not long lasting, and the interaction term approached zero within just a few years. The cumulative effects of defoliation and seasonal variation of photosynthetic capacity are illustrated in Figure 6b. At the end of the 42 years, the SPC-ON configuration would have had a 3.1% larger cumulative GPP than the SPC-OFF configuration in the absence of defoliation. However, with defoliation, it realized a 2.3% smaller cumulative GPP than the SPC-OFF configuration.

3.4. Interaction With Warming

[31] The pure effect of 4°C warming on GPP was positive in all years, and was about 3 times larger than the pure effect of seasonal variation of photosynthetic capacity (Figure 7a). Seasonally, the largest impacts (both positive) were in May and October (Figure 7b). These changes resulted from large increases in LAI (Figure 7c), and are consistent with ED2's phenology scheme (Appendix A) in that warmer temperatures are expected to lead to earlier leaf emergence in the spring and delayed leaf coloring in the fall. In June through September, higher temperatures led to slight increases in

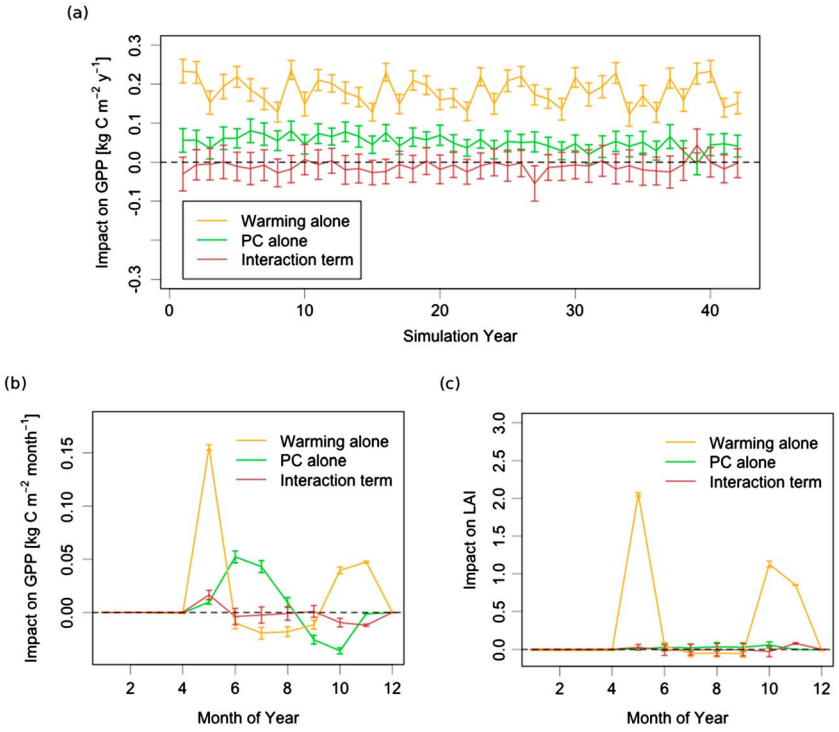

Figure 7. Impacts of 4°C warming and seasonal variation of photosynthetic capacity. Panel a: Impacts on annual gross primary productivity (GPP). Panel b: Impacts on the average annual cycle of GPP. Panel c: Impacts on the average annual cycle of leaf area index (LAI). In all panels, the solid lines show the ensemble means and the errors bars show plus and minus 1 ensemble standard deviation.

ED2's water limitation factor, and this acted to decrease GPP. The interaction term (equation (3c)) was nearly zero in most years because positive impacts in May were nearly balanced by negative impacts in October and November (Figure 7b). In May, photoperiods are relatively long, and the SPC-ON configuration has a larger photosynthetic capacity than the SPC-OFF configuration. SPC-ON is thus more sensitive to warming. The situation is reversed in the fall, when photoperiods are relatively short and SPC-ON has the smaller photosynthetic capacity (Figure 1).

4. Discussion

4.1. Model Optimization and Evaluation

[32] The estimates of $V_{cmax,s}$ obtained here (Table 3) are smaller than those reported by *Wullschleger* [1993] for *Quercus* spp. However, none of the dominant oak species at SLEF (*Q. coccinea*, *Q. velutina*, *Q. prinus*) were represented in that study. *Ashton and Berlyn* [1994] reported rates of net leaf-level photosynthesis for *Q. coccinea* and *Q. velutina* of 4.6–5.7 μmol $(m^2$ leaf $s)^{-1}$ under saturating light conditions at 25°C. Using the standard equation for Rubisco-limited photosynthesis (equation (40) of *Farquhar et al*. [1980]), this would imply a V_{cmax} value of about 16 μmol $(m^2$ leaf $s)^{-1}$. When we used an estimate of 13 μmol $(m^2$ leaf $s)^{-1}$ for $V_{cmax,s}$ (Table 3) and used the temperature dependence given in equation (1), we obtained a V_{cmax} value of about 18 μmol $(m^2$ leaf $s)^{-1}$ at 25°C, which is slightly larger than the estimate based on *Ashton and Berlyn* [1994].

[33] Overall, the SPC-ON model configuration fit NEE data collected from 2005 to 2011 at SLEF more closely than the SPC-OFF model configuration. The most pronounced differences between the model configurations occurred for gapped monthly NEE in early summer and fall (Table 4 and Figures 3b–3c). These results support the notion that V_{cmax} should be sensitive to photoperiod [*Bauerle et al*., 2012; *Stoy et al*., 2013]. Methods exist for quantifying the levels of support that should be associated with different model formulations [*Jeong et al*., 2012], but we did not pursue this here because these methods can be computationally expensive and the preference for SPC-ON seemed unambiguous (Table 4). However, these methods may be useful if future analyses consider models of V_{cmax} seasonality with more subtle differences than those considered here.

4.2. Comparison to Other Models With Seasonal Variation of Photosynthetic Capacity

[34] Models of leaf-gas exchange have shown that including seasonal variation of photosynthetic capacity greatly improves seasonal simulations of leaf-level CO_2 flux [*Wilson et al*., 2001; *Kosugi et al*., 2003; *Wang et al*., 2003]. Process-based models of grassland CO_2 exchange have also been shown to require seasonal variation of photosynthetic capacity [*Wolf et al*., 2006]. Our work explores the longer-term implications of these findings by using a comprehensive terrestrial biosphere model capable of simulating changes in temperate forest ecosystem structure, composition, and functioning.

[35] Seasonal variation of photosynthetic capacity for broadleaf deciduous plant functional types has recently been incorporated in the Community Land Model (CLM) [*Oleson et al*., 2010]. *Bonan et al*. [2011] used CLM to compare global simulations with and without seasonal variation of photosynthetic capacity. In these simulations, they used the same summer solstice value of V_{cmax} ($V_{cmax,s}$ in our notation). Thus, their simulation without seasonal variation of photosynthetic capacity always had a photosynthetic capacity that was greater than or equal to their simulation that included seasonal variation of photosynthetic capacity. Including seasonal reductions in photosynthetic capacity reduced their simulated global GPP by about 8%. In another study using CLM, *Bauerle et al*. [2012] also simulated reductions in GPP owing to seasonal variation of photosynthetic capacity. We found the opposite response: in our simulations of SLEF, seasonal variation of photosynthetic capacity caused GPP to increase by about 3%. Our simulations were different because our estimates for $V_{cmax,s}$ were conditional on model configuration. Consequently, our SPC-ON configuration had a larger photosynthetic capacity than our SPC-OFF configuration in late spring/early summer, and vice versa in the fall (Figure 1).

4.3. Implications for Ecosystem Carbon Budgets

[36] It is not possible to completely "tune away" the impacts of seasonal variation of photosynthetic capacity, especially if there is temporal correlation between photosynthetic capacity and climate anomalies or disturbances. We simulated a disproportionate effect of gypsy moth defoliation on the SPC-ON configuration because the defoliation peaked in June, when SPC-ON has its largest photosynthetic capacity (at a given temperature). The interaction term between seasonal variation of photosynthetic capacity and defoliation attained its largest values in the few years following defoliation (Figure 6). Although our simulations highlight the recovery from a single defoliation event, it would also be of interest in future work to investigate how this interaction term would respond to repeated defoliations. Gypsy moth outbreaks in North America are cyclical with primary periodicities of about 5 and 10 years [*Johnson et al*., 2006], and a previous modeling study pointed out nonlinear ecosystem responses to changes in defoliation periodicity and intensity [*Medvigy et al*., 2012].

[37] Although our results were based on a single site, gypsy moth is now ubiquitous in forests of the Mid-Atlantic region. Approximately 24% of forests in the region are classified as highly susceptible to gypsy moth, and 7% are classified as extremely susceptible [*Liebhold et al*., 1992; *USDA Forest Service*, 2009]. In New Jersey, 36% of forests are classified as highly susceptible to gypsy moth defoliation and 15% are classified as extremely susceptible.

[38] Our results can also help inform how defoliation by other insects interacts with seasonal variation of photosynthetic capacity. For example, forest tent caterpillar (*Malacosoma disstria* Hubner) is another major defoliator of deciduous tree species in North America [*Churchill et al*., 1964; *Man and Rice*, 2010], and also defoliates in the beginning of the growing season when the SPC-ON configuration has its largest photosynthetic capacity. Understanding the interplay between seasonal variation of photosynthetic capacity (and phenology in general) and insect disturbances will become increasingly important if insect disturbances become more frequent with climate change, as some studies have suggested [*Kurz et al*., 2008; *Bentz et al*., 2010; *Sturrock et al*., 2011].

[39] Seasonal variation of photosynthetic capacity may also modulate the effect of global warming on ecosystem functioning. Over the past few decades, spring and autumn

temperatures have risen by 1.1°C and 0.8°C, respectively, over northern latitudes worldwide [*Mitchell and Jones*, 2005]. Analyzing atmospheric CO_2 records and eddy-flux measurements for the same northern latitudes, *Piao et al*. [2008] found that warming increased respiration more than photosynthesis in the fall, but not in the spring. As they argued, part of the explanation for this is likely due to the different temperature sensitivities of respiration and photosynthesis. However, seasonal variation of photosynthetic capacity may also be playing a role, causing a larger enhancement of GPP in the spring and a smaller enhancement of GPP in the fall.

[40] Different amounts of warming in the spring and fall have occurred on continental and smaller scales [*Mitchell and Jones*, 2005]. Eurasia in particular has warmed more in the spring than in the fall, and North America has warmed more in the fall than in the spring. Other things being equal, our results suggest that seasonal variation of photosynthetic capacity would have caused Eurasia to have the stronger GPP response to warming. Interestingly, the enhanced greening pattern seen in remote sensing data has been more significant and coherent in Eurasia than in North America [*Zhou et al*., 2001].

4.4. Uncertainties and Areas for Future Work

[41] The primary purpose of this study was to identify conditions under which seasonal variation of photosynthetic capacity is likely to be important. To first order, this can be done with any prescription that gives a relatively larger V_{cmax} at the beginning of the growing season and relatively smaller V_{cmax} at the end of the growing season (Figure 1). We selected the particular functional form given by equation (2) because it is simple, scalable to other sites, and has some support from previous observations [*Bauerle et al*., 2012]. Other approaches to parameterizing the seasonality of V_{cmax} could have been taken, though all would have their own advantages and disadvantages. For example, we could have taken a semi-empirical approach, dispensing with equation (2) altogether and instead estimating a different V_{cmax} for each month of the year [*Wolf et al*., 2006]. This may provide a finer temporal resolution of the seasonal cycle of V_{cmax} (provided parameter uncertainties are not too large), but it would also increase the number of estimated parameters, increasing the complexity of the model and of the optimization process. Furthermore, there would be no obvious way to scale to other sites (whereas equation (2) scales using photoperiod). We therefore advocate for the development in future studies of more mechanistic models of seasonality in V_{cmax} with relatively small numbers of parameters. Testing such models across temperate and boreal biomes may now be possible using the FLUXNET database [*Stoy et al*., 2013].

[42] *Bonan et al*. [2011] pointed out the importance of the V_{cmax} parameter for simulating GPP, and argued that model structural errors can be partially compensated for by adjusting this parameter. This is manifest in our results. Use of a larger value of $V_{cmax,s}$ in our SPC-ON configuration than in our SPC-OFF configuration allows the two configurations to simulate similar annual GPP. However, on subannual time scales the differences between these model configurations are more apparent. This partial compensation in annual GPP would not have been obtained if we had not included annual data as a constraint on the model. Our decision to weight both monthly and annual observations in parameterizing the model (Appendix A) is consistent with our intention that ED2 be capable of simulating multiple time scales.

[43] This study considered a single stand in the New Jersey Pinelands. This highly instrumented, intermediate-aged stand is representative of oak/pine communities on the eastern US Atlantic coastal plain [*McCormick and Jones*, 1973; *Lathrop and Kaplan*, 2004; *Skowronski et al*., 2007]. Other typical upland forest communities on the Atlantic coastal plain include mixed pine/oak stands with pitch pine and mixed oaks in the overstory, and pine/scrub oak stands dominated by pitch pine with scrub oaks in the understory [*Skowronski et al*., 2007]. Because pines are an important component of these other community types, assessment of the ecosystem-level effects of seasonal variation of photosynthetic capacity would require understanding of seasonal variation of pine photosynthetic capacity. This represents an interesting challenge for future modeling studies. Pitch pine flushes one cohort of needles per year, but holds two cohorts through the peak of the growing season. It would thus be important to track the photosynthetic capacity of multiple cohorts of needles. Only a few terrestrial biosphere models currently have this functionality [e.g., *Ogée et al*., 2003]. An additional complicating factor is the seasonal variation of LAI. In pine stands in the New Jersey Pine Barrens, the LAI of evergreen needleleaf trees is typically twice as large in the summer as in the winter [*Clark et al*., 2012]. Seasonal variations in LAI have also been reported for temperate evergreen needleleaf stands from Oregon [*Spanner et al*., 1994] to Florida [*Powell et al*., 2005]. However, this variation has seldom been represented in models.

[44] Finally, it would also be interesting to consider the interplay between seasonal variation of photosynthetic capacity and nutrient dynamics. Implementation of nitrogen and phosphorus cycles in ED2 is currently a work in progress.

5. Conclusions

[45] We used model simulations to understand how seasonal variation of photosynthetic capacity affected gross primary productivity on monthly to multidecadal time scales at a representative oak/pine forest on the Atlantic coastal plain of the eastern US. Including this variation had a large impact on model simulations of subannual time scales. It also affected the simulation of processes that are linked to the annual cycle, including defoliation, budburst, and leaf coloration. While seasonal variation of photosynthetic capacity should be included in models, care is required because models may require reparameterization to ensure that their ability to simulate annual and longer time scales is not degraded. Continued assessment of the impacts of seasonal variation of photosynthetic capacity on ecosystem composition, structure, and functioning remains an important task for our understanding of short- and long-term behavior of these systems, their responses to environmental variability, and their responses to disturbances.

Appendix A: Model Configuration

[46] Before carrying out the Markov chain Monte Carlo, we applied three changes in model structure affecting leaf area dynamics, allometries, and heterotrophic respiration. Leaf emergence in the spring was parameterized according to *Jeong et al*. [2013]. This parameterization was developed

using a ~20 year record of observations at Harvard Forest [*O'Keefe*, 2000] and a ~3 year record of observations from 196 measurement sites located throughout the US from the USA National Phenology Network [*USA National Phenology Network*, 2011]. A parameterization for leaf coloration in the fall using Harvard Forest and USA National Phenology Network data has also been recently developed (S.-J. Jeong, manuscript in preparation, 2013) and has been implemented here. Allometries for our oak and pine PFTs were taken from *Whittaker and Woodwell* [1968], who determined allometric relationships for the species characteristic of the northeastern US Atlantic coastal plain. Specifically, we used their *Quercus coccinea* allometry for our oak PFT and their *Pinus rigida* allometry for our pine PFT. Finally, to simulate heterotrophic respiration, we replaced the empirical scheme that has previously been used in ED2 [*Medvigy et al*., 2009] with the more mechanistic Dual Arrhenius and Michaelis-Menten kinetics (DAMM) scheme introduced by *Davidson et al*. [2012].

[47] Although previous ED2 simulations have successfully simulated many mesic sites in the eastern US [*Medvigy et al*., 2009; *Medvigy and Moorcroft*, 2012], we found that SLEF, with its relatively xeric soils, was poorly simulated for all choices of $V_{cmax,s}$. In particular, we were unable to simultaneously simulate the observed maximum summer drawdown of NEE, the diurnal cycle of NEE, overall tree growth, and overall tree mortality. We therefore broadened the scope of our model optimization to include four parameters: oak $V_{cmax,s}$ (a control on photosynthesis), oak fine root turnover rate (T_{root}; a control on net primary production), the baseline heterotrophic respiration rate (a control on heterotrophic respiration; the actual parameter is denoted α_{sx} in *Davidson et al*. [2012]), and the slope of the relationship between leaf-level stomatal conductance and CO_2 flux (M; a control on the diurnal cycle of photosynthesis; see equation (B15) of *Medvigy et al*. [2009]). Pine-specific parameters were not selected because there is only a small amount of pine in the stand (Figure 2). We did not wish to express an a priori preference for either of the SPC-ON or SPC-OFF model configurations, and so the four-parameter Markov chain Monte Carlo was carried out for both configurations.

[48] Prior probability density functions for the parameters were assumed to be independent and were taken to be gamma distributions because all parameters are positive definite. Expected values of the prior distributions were taken from the standard parameterizations of ED2 [*Medvigy et al*., 2009] and DAMM [*Davidson et al*., 2012]. Standard deviations of the prior distributions were taken to be about 10 times the parameter uncertainties reported in *Medvigy et al*. [2009] in order to generate noncommittal priors. In our analysis, the main function of the prior was to keep the parameters from becoming negative.

[49] The model parameterizations were developed using data only from 2006. We used the following data sets to parameterize the model: (i) half-hourly gapped NEE, (ii) monthly gapped net ecosystem exchange, (iii) monthly gapped nighttime-only NEE, (iv) annual gapped NEE, (v) annual gapped nighttime NEE, (vi) total annual basal area increment (BAI) of all hardwood trees in the measurement plot, (vii) total annual BAI of all conifer trees in the measurement plot, (viii) total annual mortality of all hardwood trees in the measurement plot, and (ix) total annual mortality of all conifer trees in the measurement plot. The gapped NEE includes only the NEE values that were actually observed and passed quality control. They do not represent the total ecosystem-atmosphere exchanges because there are missing values in the time series of measurements; consequently, these sums differ from those reported previously [*Clark et al*., 2010]. The advantage of this approach is that it eliminates uncertainties that may be present in gap-filling algorithms [*Falge et al*., 2001]. Taken together, these data sets represent a range of time scales. This is important because previous work has shown that it is possible for models to perform reasonably well at one time scale while performing poorly at other time scales [*Braswell et al*., 2005; *Medvigy et al*., 2009]. Our approach allows for simultaneous constraints on all time scales.

[50] The likelihood function quantifies the model-data mismatch. For the half-hourly NEE, we took the double-exponential distribution of *Hollinger and Richardson* [2005] to describe observational errors. We then repeatedly sampled from this distribution to estimate errors associated with monthly and yearly gapped NEE. We estimated errors for the tree growth and mortality data sets by bootstrapping. We computed an overall log likelihood (LL) by combining the log likelihoods corresponding to individual data sets [*Medvigy et al*., 2009; *Kim et al*., 2012]:

$$LL = \sum_{i=1}^{9} w_i LL_i. \tag{A1}$$

[51] Here, LL_i is the log likelihood of one of the nine data sets and w_i is a weighting factor. Weighted log likelihood values that are closer to 0 represent a closer match to the observations. Because the ED2 model is intended to generate predictions across a wide range of time scales, we decided to give equal weighting to the half-hourly, monthly, and yearly data. With N_{hh} representing the total number of elements in data set (i), N_m representing the total number of elements in data sets (ii) and (iii) combined, and N_y representing the total number of elements in data sets (iv)–(ix) combined, we chose:

$$\mathrm{w}_i = \begin{cases} \dfrac{N_y}{N_{hh}} & i = 1 \\ \dfrac{N_y}{N_m} & i = 2, 3 \\ 1 & i > 3 \end{cases} \tag{A2}$$

[52] We carried out over 400,000 simulations of the period 2005–2006 by running 20 parallel runs, each of at least 20,000 iterations. Data from 2005 were discarded as spin-up and data from 2006 were used to constrain the model. To ensure a consistent comparison with gapped observations, we computed the corresponding gapped fluxes from the simulations.

[53] **Acknowledgments.** We gratefully acknowledge support from USDA joint venture agreement 10-JV-11242306-136 and Office of Science (BER), US Department of Energy DE-SC0007041 award NA08OAR4320752 from the National Oceanic and Atmospheric Administration, U.S. Department of Commerce. Simulations presented here were performed on computational resources supported by the PICSciE-OIT High Performance Computing Center and Visualization Laboratory at Princeton University. We are grateful to two anonymous reviewers whose comments significantly improved the quality of the original manuscript.

References

Ashton, P. M. S., and G. P. Berlyn (1994), A comparison of leaf physiology and anatomy of Quercus (Section Erythrobalanus-Fagaceae) species in different light environments, *Am. J. Bot.*, *81*, 589–597.

Bauerle, W. L., R. Oren, D. A. Way, S. S. Qian, P. C. Stoy, P. E. Thornton, J. D. Bowden, F. M. Hoffman, and R. F. Reynolds (2012), Photoperiodic regulation of the seasonal pattern of photosynthetic capacity and the implications for carbon cycling, *Proc. Natl. Acad. Sci. U. S. A.*, *109*, 8612–8617.

Bentz, B. J., J. Régnière, C. J. Fettig, E. M. Hansen, J. L. Hayes, J. A. Hicke, and S. J. Seybold (2010), Climate change and bark beetles of the western United States and Canada: Direct and indirect effects, *BioScience*, *60*, 602–613.

Bonan, G. B. (2008), *Ecological Climatology: Concepts and Applications*, 2nd ed., Cambridge Univ. Press, Cambridge, U. K.

Bonan, G. B., P. J. Lawrence, K. W. Oleson, S. Levis, M. Jung, M. Reichstein, D. M. Lawrence, and S. C. Swenson (2011), Improving canopy processes in the Community Land Model version 4 (CLM4) using global flux fields empirically inferred from FLUXNET data, *J. Geophys. Res.*, *116*, G02014, doi:10.1029/2010JG001593.

Braswell, B. H., W. J. Sacks, E. Linder, and D. S. Schimel (2005), Estimating diurnal to annual ecosystem parameters by synthesis of a carbon flux model with eddy covariance net ecosystem exchange observations, *Global Change Biology*, *11*, 335–355.

Churchill, G. B., H. H. John, D. P. Duncan, and A. C. Hodson (1964), Long-term effects of defoliation of aspen by the forest tent caterpillar, *Ecology*, *45*, 630–636.

Clark, K. L., N. Skowronski, and J. Hom (2010), Invasive insects impact forest carbon dynamics, *Global Change Biology*, *16*, 88–101.

Clark, K. L., N. Skowronski, M. Gallagher, H. Renninger, and K. Schäfer (2012), Effects of invasive insects and fire on forest energy exchange and evapotranspiration in the New Jersey pinelands, *Agric. For. Meteorol.*, *166–167*, 50–61.

Davidson, E. A., S. Samanta, S. S. Caramori, and K. Savage (2012), The Dual Arrhenius and Michaelis-Menten kinetics model for decomposition of soil organic matter at hourly to seasonal time scales, *Global Change Biology*, *18*, 371–384.

Falge, E., et al. (2001), Gap filling strategies for defensible annual sums of net ecosystem exchange, *Agric. For. Meteorol.*, *107*, 43–69.

Farquhar, G. D., S. von Caemmerer, and J. A. Berry (1980), A biochemical model of photosynthetic CO_2 assimilation in leaves of C_3 species, *Planta*, *149*, 78–90.

Fox, A., et al. (2009), The REFLEX project: Comparing different algorithms and implementations for the inversion of a terrestrial ecosystem model against eddy covariance data, *Agric. For. Meteorol.*, *149*, 1597–1615.

Grassi, G., E. Vicinelli, F. Ponti, L. Cantoni, and F. Magnani (2005), Seasonal and interannual variability of photosynthetic capacity in relation to leaf nitrogen in a deciduous forest plantation in northern Italy, *Tree Physiol.*, *25*, 349–360.

Hollinger, D. Y., and A. D. Richardson (2005), Uncertainty in eddy covariance measurements and its application to physiological models, *Tree Physiol.*, *25*, 873–885.

Jeong, S.-J., D. Medvigy, E. Shevliakova, and S. Malyshev (2012), Uncertainties in terrestrial carbon budgets related to spring phenology, *J. Geophys. Res.*, *117*, G01030, doi:10.1029/2011JG001868.

Jeong, S.-J., D. Medvigy, E. Shevliakova, and S. Malyshev (2013), Impacts of projected climate warming on the "green wave" of springtime budburst in the U.S., *Geophys. Res. Lett.*, *40*, 359–364, doi:10.1029/2012GL054431.

Johnson, D. M., A. M. Liebhold, O. N. Bjørnstad, and M. L. McManus (2005), Circumpolar variation in periodicity and synchrony among gypsy moth populations, *J. Anim. Ecol.*, *74*, 882–892.

Johnson, D. M., A. M. Liebhold, and O. N. Bjørnstad (2006), Geographical variation in the periodicity of gypsy moth outbreaks, *Ecography*, *29*, 367–374.

Kim, Y., R. G. Knox, M. Longo, D. Medvigy, L. R. Hutyra, E. H. Pyle, S. C. Wofsy, R. L. Bras, and P. R. Moorcroft (2012), Seasonal carbon dynamics and water fluxes in an Amazon rainforest, *Global Change Biology*, *18*, 1322–1334, doi:10.1111/j.1365-2486.2011.02629.x.

Knorr, W., and J. Kattge (2005), Inversion of terrestrial ecosystem model parameter values against eddy covariance measurements by Monte Carlo sampling, *Global Change Biology*, *11*, 1333–1351.

Kosugi, Y., S. Shibata, and S. Kobashi (2003), Parameterization of the CO_2 and H_2O gas exchange of several temperate deciduous broad-leaved trees at the leaf scale considering seasonal changes, *Plant Cell Environ.*, *26*, 285–301.

Krinner, G., N. Viovy, N. de Noblet-Ducoudré, J. Ogée, J. Polcher, P. Friedlingstein, P. Ciais, S. Sitch, and I. C. Prentice (2005), A dynamic global vegetation model for studies of the coupled atmosphere-biosphere system, *Global Biogeochem. Cycles*, *19*, GB1015, doi:10.1029/2003GB002199.

Kurz, W. A., C. C. Dymond, G. Stinson, G. J. Rampley, E. T. Neilson, A. L. Carroll, and L. Safranyik (2008), Mountain pine beetle and forest carbon feedback to climate change, *Nature*, *452*, 987–990.

Lathrop, R., and K. B. Kaplan (2004), New Jersey Land Use/Land Cover Update: 2000–2001, Department of Environmental Protection, NJ, p. 35.

Lebourgeois, F., J.-C. Pierrat, V. Perez, C. Piedallu, S. Cecchini, and E. Ulrich (2010), Simulating phenological shifts in French temperate forests under two climatic change scenarios and four driving global circulation models, *Int. J. Biometeorol.*, *54*, 563–581.

Liebhold, A. M., J. A. Halverson, and G. A. Elmes (1992), Gypsy moth invasion in North America: a quantitative analysis, *J. Biogeogr.*, *19*, 513–520.

Man, R., and J. A. Rice (2010), Response of aspen stands to forest tent caterpillar defoliation and subsequent overstory mortality in northwestern Ontario, Canada, *For. Ecol. Manage.*, *26*, 1853–1860.

McCormick, J., and L. Jones (1973), The Pine Barrens: Vegetation Geography. New Jersey State Museum, p. 76, Research Report Number 3.

Medvigy, D., and P. R. Moorcroft (2012), Regional scale prediction of forest dynamics: Evaluation of a terrestrial biosphere model for northeastern U.S. forests, *Philos. Trans. R. Soc., B*, *367*, 222–235.

Medvigy, D., S. C. Wofsy, J. W. Munger, D. Y. Hollinger, and P. R. Moorcroft (2009), Mechanistic scaling of ecosystem function and dynamics in space and time: Ecosystem demography model version 2, *J. Geophys. Res.*, *114*, G01002, doi:10.1029/2008JG000812.

Medvigy, D., K. L. Clark, N. S. Skowronski, and K. V. R. Schäfer (2012), Simulated impacts of insect defoliation on forest carbon dynamics, *Environ. Res. Lett.*, *7*, 045703, doi:10.1088/1748-9326/7/4/045703.

Meehl, G. A., et al. (2007), Global Climate Projections, in *Climate Change 2007: The Physical Science Basis. Contribution of Working Group I to the Fourth Assessment Report of the Intergovernmental Panel on Climate Change*, edited by S. Solomon et al., pp. 747–845, Cambridge Univ. Press, Cambridge, United Kingdom and New York, NY, USA.

Menzel, A., N. Estrella, W. Heitland, A. Susnik, C. Schleip, and V. Dose (2008), Bayesian analysis of the species-specific lengthening of the growing season in two European countries and the influence of an insect pest, *Int. J. Biometeorol.*, *52*, 209–218.

Migliavacca, M., O. Sonnentag, T. F. Keenan, A. Cescatti, J. O'Keefe, and A. D. Richardson (2012), On the uncertainty of phenological responses to climate change, and implications for a terrestrial biosphere model, *Biogeosciences*, *9*, 2063–2083.

Mitchell, T. D., and P. D. Jones (2005), An improved method of constructing a database of monthly climate observations and associated high-resolution grids, *Int. J. Climatol.*, *25*, 693–712.

O'Keefe, J. (2000), Phenology of woody species, Harvard Forest Data Archive: HF003, available at http://harvardforest.fas.harvard.edu:8080/exist/xquery/data.xq?id=hf003, Harvard Univ., Cambridge, Mass.

Ogée, J., Y. Brunet, D. Loustau, P. Berbigier, and S. Delzon (2003), *MuSICA*, a CO_2, water and energy multilayer, multileaf pine forest model: Evaluation from hourly to yearly time scales and sensitivity analysis, *Global Change Biology*, *9*, 697–717.

Oleson, K. W., et al. (2010), Technical description of version 4.0 of the Community Land Model (CLM). NCAR Technical Note NCAR/TN-478 +STR.

Ow, L. F., D. Whitehead, A. S. Walcroft, and M. H. Turnbull (2010), Seasonal variation in foliar carbon exchange in *Pinus radiata* and *Populus deltoides*: Respiration acclimates fully to changes in temperature but photosynthesis does not, *Global Change Biology*, *16*, 288–302.

Piao, S., et al. (2008), Net carbon dioxide losses of northern ecosystems in response to autumn warming, *Nature*, *451*, 49–53.

Powell, T. L., G. Starr, K. L. Clark, T. A. Martin, and H. L. Gholz (2005), Ecosystem and understory water and energy exchange for a mature, naturally regenerated pine flatwoods forest in north Florida, *Can. J. For. Res.*, *35*, 1568–1580.

Richardson, A. D., and D. Y. Hollinger (2005), Statistical modeling of ecosystem respiration using eddy covariance data: maximum likelihood parameter estimation, and Monte Carlo simulation of model and parameter uncertainty, applied to three simple models, *Agric. For. Meteorol.*, *131*, 191–208.

Richardson, A., et al. (2010), Estimating parameters of a forest ecosystem C model with measurements of stocks and fluxes as joint constraints, *Oecologia*, *164*, 25–40.

Richardson, A. D., T. F. Keenan, M. Migliavacca, Y. Ryu, O. Sonnentag, and M. Toomey (2013), Climate change, phenology, and phenological control of vegetation feedbacks to the climate system, *Agric. For. Meteorol.*, *169*, 156–173.

Schäfer, K. V. R. (2011), Canopy stomatal conductance following drought, disturbance and death in an upland oak/pine forest of the New Jersey Pine Barrens, USA, *Front. Plant Sci.*, *2*, 1–7.

Schäfer, K. V. R., K. L. Clark, N. Skowronski, and E. P. Hamerlynck (2010), Impact of insect defoliation on forest carbon balance as assessed with a canopy assimilation model, *Global Change Biology*, *16*, 546–560.

Seager, R., M. Ting, C. Li, N. Naik, B. Cook, J. Nakamura, and H. Liu (2013), Projections of declining surface-water availability for the southwestern United States, *Nat. Clim. Change*, *3*, 482–486.

Skowronski, N., K. Clark, R. Nelson, J. Hom, and M. Patterson (2007), Remotely sensed measurements of forest structure and fuel loads in the Pinelands of New Jersey, *Remote Sens. Environ.*, *108*, 123–129.

Spanner, M., L. Johnson, J. Miller, R. McCreight, J. Freemantle, J. Runyon, and P. Gong (1994), Remote sensing of seasonal leaf area index across the Oregon transect, *Ecol. Appl.*, *4*, 258–271.

Stoy, P. C., A. M. Trowbridge, and W. L. Bauerle (2013), Controls on seasonal patterns of maximum ecosystem carbon uptake and canopy-scale photosynthetic light response: Contributions from both temperature and photoperiod, *Photosyn. Res.*, doi:10.1007/s11120-013-9799-0.

Sturrock, R. N., S. J. Frankel, A. V. Brown, P. E. Hennon, J. T. Kliejunas, K. J. Lewis, and A. J. Woods (2011), Climate change and forest diseases, *Plant Pathol.*, *60*, 133–149.

Trudinger, C. M., et al. (2007), OptIC project: an intercomparison of optimization techniques for parameter estimation in terrestrial biogeochemical models, *J. Geophys. Res.*, *112*, G02027, doi:10.1029/2006JG000367.

USA National Phenology Network (2011), USA-NPN, Tuscon, Arizona, USA. Data set accessed 2012-05-30 at http://www.usanpn.org/results/data.

USDA Forest Service (2009), *Major Forest Insect and Disease Conditions in the United States 2007*, USDA Forest Service, Forest Health Protection, Washington, D. C.

Vitasse, Y., C. Francois, N. Delpierre, E. Dufrene, A. Kremer, I. Chuine, and S. Delzon (2011), Assessing the effects of climate change on the phenology of European temperate trees, *Agric. For. Meteorol.*, *151*, 969–980.

Wang, Q., J. Tenhunen, E. Falge, C. Bernhofer, and A. Granier (2003), Simulation and scaling of temporal variation in gross primary production for coniferous and deciduous temperate forests, *Global Change Biology*, *10*, 37–51.

Wang, Q., A. Iio, J. Tenhunen, and Y. Kakubari (2008), Annual and seasonal variations in photosynthetic capacity of *Fagus crenata* along an elevation gradient in the Naeba Mountains, Japan, *Tree Physiol.*, *28*, 277–285.

Whittaker, R. H., and G. M. Woodwell (1968), Dimension and production relations of trees and shrubs in the Brookhaven Forest, New York, *J. Ecol.*, *56*, 1–25.

Wilson, K. B., D. D. Baldocchi, and P. J. Hanson (2001), Leaf age affects the seasonal pattern of photosynthetic capacity and net ecosystem exchange of carbon in a deciduous forest, *Plant Cell Environ.*, *24*, 571–583.

Wolf, A., K. Akshalov, N. Saliendra, D. A. Johnson, and E. A. Laca (2006), Inverse estimation of Vc_{max}, leaf area index, and the Ball-Berry parameter from carbon and energy fluxes, *J. Geophys. Res.*, *111*, D08S08, doi:10.1029/2005JD005927.

Wullschleger, S. D. (1993), Biochemical limitation to carbon assimilation in C_3 plants – A retrospective analysis of the A/C_i curves from 109 species, *J. Exp. Bot.*, *44*, 907–920.

Xu, L., and D. D. Baldocchi (2003), Seasonal trends in photosynthetic parameters and stomatal conductance of blue oak (*Quercus douglasii*) under prolonged summer drought and high temperature, *Tree Physiol.*, *23*, 865–877.

Zhou, L. M., et al. (2001), Variations in northern vegetation activity inferred from satellite data of vegetation index during 1981 to 1999, *J. Geophys. Res.*, *106*, 20,069–20,083.